—Original—

Finite Element Analysis of the Effect of Femoral Prosthesis Varus and Valgus Angle Installation on the Lateral Compartment in Unicompartmental Knee Arthroplasty

Yonggui Wang[1,2], Chongyang Xu[1], Bo Yang[1], Fei Yu[1] and Ai Guo[1]

[1]Department of Orthopedic Surgery, Beijing Friendship Hospital, Capital Medical University, Beijing, China
[2]Department of Orthopedics, Xiangyang No. 1 People's Hospital, Hubei University of Medicine, Xiangyang, China

Background: This study used finite element analysis (FEA) to investigate the effect of varus and valgus angle on the lateral compartment in unicompartmental knee arthroplasty (UKA).

Methods: One patient who underwent UKA was enrolled as the subject. Thirteen working conditions of the femoral prosthesis were simulated at varus and valgus angles of 0°, 2°, 4°, 6°, 8°, 10°, and 12°. A load of 1,000 N was applied downward along the mechanical axis of the femur, and the highest stress values on the surface of the polyethylene liner, cancellous bone under the tibial prosthesis, cartilage of femur lateral condyle, lateral meniscus, and tibial lateral plateau cartilage in each model were recorded. The six highest points were used to calculate the mean value.

Results: The highest stress values on the surface of the polyethylene liner, cancellous bone under the tibial prosthesis, cartilage of femur lateral condyle, lateral meniscus, and tibial lateral plateau cartilage increased with an increase in the femoral prosthesis varus/valgus angle. As compared with the standard position of the femoral prosthesis, there was no significant difference in the surface stress values of the polyethylene liner, cancellous bone under the tibial prosthesis, cartilage of femur lateral condyle, lateral meniscus and tibial lateral plateau cartilage when the femoral prosthesis varus/valgus angle was less than 4° ($p > 0.05$). In addition, the stress magnitude on the polyethylene liner, cancellous bone under the tibial prosthesis, cartilage of femur lateral condyle, lateral meniscus, and tibial lateral plateau cartilage significantly increased when the femoral prosthesis varus/valgus angle was greater than 4° ($p < 0.001$).

Conclusions: The optimal femoral prosthesis varus/valgus angle in UKA was less than 4°.

(J Nippon Med Sch 2024; 91: 88–98)

Key words: anteromedial osteoarthritis (AMOA), femoral prosthesis, biomechanical research

Introduction

Knee osteoarthritis is the most common form of osteoarthritis in clinical practice. Unicompartmental knee arthroplasty (UKA) is an effective surgical treatment for single-compartment osteoarthritis of the knee joint. It has been widely applied by orthopedists because it is associated with less trauma, shorter operation time, less bleeding, less interference to soft tissues around the knee joint, and faster recovery after surgery[1–3]. Numerous studies have reported excellent success rates for UKA: from 85% to 95% at the 10-year mark[4,5]. Nevertheless, despite these favorable outcomes, the issue of abnormal stress distribution within the knee joint resulting from suboptimal prosthesis placement during surgery continues to pose a challenge. Misalignment can lead to prosthesis loosening and progression of osteoarthritis in the contralateral compartment and patellofemoral compartment[6–10]. Because of the wide use of finite element analysis (FEA) in orthope-

Correspondence to Ai Guo, Department of Orthopedic Surgery, Beijing Friendship Hospital, Capital Medical University, 95 Yong'an Road, Xicheng District, Beijing 100050, China
E-mail: guoai2@yeah.net
https://doi.org/10.1272/jnms.JNMS.2024_91-110
Journal Website (https://www.nms.ac.jp/sh/jnms/)

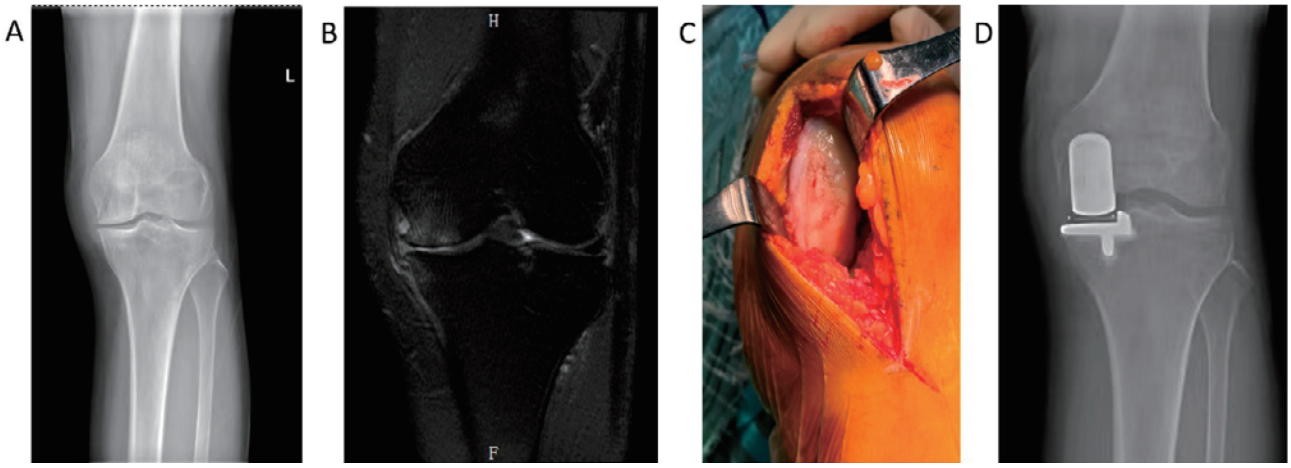

Fig. 1 Imaging findings from the patient. **(A)** Preoperative radiograph of the knee. **(B)** Preoperative MRI of the knee. **(C)** Intraoperative photograph showing severe degeneration of femoral lateral condylar cartilage. **(D)** Postoperative radiograph of the knee.

dic biomechanical research, an increasing number of studies are using FEA to examine changes in knee biomechanics after UKA.

Researchers in China and other countries[11–13] have used FEA to study the effect of UKA on knee biomechanics. However, the enrollment of healthy adult volunteers as research subjects is a major limitation of these studies, as results obtained from FEA of healthy knee joints may not accurately reflect the biomechanics of knee joints affected by osteoarthritis. In addition, these studies have focused more on internal eversion and posterior inclination of tibial prosthesis during UKA, with relatively little attention paid to femoral prosthesis internal and external eversion[14,15].

Given these limitations of previous studies, it is necessary to adopt a more accurate FEA modeling method to study changes in knee biomechanics after UKA. We hypothesized that selecting a patient after UKA as a research subject of FEA—with the study performed in 2-degree intervals and evaluating the effect of different varus/valgus angles of the femoral prosthesis on knee biomechanics—would yield more reliable results on changes in knee biomechanics after UKA.

Materials and Methods

Study Participant

A patient who had undergone UKA was selected as the subject for the FEA model. Image data of the patient are shown in **Figure 1A～D**. The patient was a 68-year-old woman with a body mass index of 25.7 kg/m^2. After excluding other joint diseases, we diagnosed anteromedial osteoarthritis in May 2020, and she underwent a mobile-bearing UKA. After the operation, the placement angle of the UKA prosthesis was measured.

The protocol of this study was approved by the ethics committee of Xiangyang No. 1 People's Hospital (XYYYE 20220023). All clinical investigations were performed in accordance with the principles of the Declaration of Helsinki. The patient was informed that relevant data were being considered for submission in an anonymized form and she consented.

Research Tools and Image Acquisition Equipment

A 64-row computed tomography (CT) scanner (Siemens, Germany) and a 3.0-T magnetic resonance imaging system (Philips, Netherlands) were used.

Computer Processing Software

The software Mimics Medical 21.0 (Materialise, Geomagic Studio 2013; 3D Systems, USA), Solidworks 2017 (Dassault Systemes), and ANSYS Workbench 2019 (ANSYS) were used for medical modeling, 3D modeling, and FEA, respectively. SPSS software, version 18.0, was used for statistical analysis.

Storage of Scanned Images

A full-length plain scan of both lower extremities was performed with a layer thickness of 0.6 mm by using a 64-row CT scanner (Siemens, Germany). The patient's right knee, including 15 cm each of the distal femur and proximal tibia, was scanned using the 3.0-T magnetic resonance imaging system (Philips, the Netherlands). Finally, the imaging data were stored in a CD-ROM in the DICOM format.

Prosthetic Materials

A third-generation Oxford unicondyle mobile-bearing prosthesis was used for UKA.

Data Import and Data Processing

The thin-slice CT data of the knee joint stored in DICOM format were loaded into Mimics Medical 21.0 software to check the accuracy and consistency of the anterior-posterior, superior-inferior, and left-right directions displayed by the CT data with the actual knee joint. Two-dimensional tomography images of the knee joint were then generated in different views, including coronal, sagittal, and axial views. To generate a comprehensive 3D model of the knee bone, the software's masking tool was used with predefined threshold values to extract an initial rough knee bone model. Subsequently, manual editing techniques, including area growth, separation mask, edit mask, and cavity filling, were used to refine and enhance the model's accuracy and completeness. The computational part function was used to generate a 3D reconstruction based on the extracted skeletal model, which was then converted into STL format and exported. The process of reconstructing 3D models of soft tissues based on MRI 2D images was basically the same as the method for CT images. MRI data were imported into Mimics Medical 21.0 software. Next, utilizing the aforementioned software tools, preliminary 3D models of soft tissues, including the articular cartilage and meniscus, were meticulously extracted, manually edited, and carefully trimmed. Finally, the rough 3D models were reconstructed in 3D using the computational parts function to generate STL format files, which were exported for further analysis.

Reverse Modeling to Generate Solid 3D Data

The STL format files of each structure of knee bone and soft tissue generated above were imported into the Geomagic Studio 2013 software. Tools such as regrid, noise reduction, fast smoothing, nail removal, feature removal, grid doctor were used to improve the quality of STL triangular surface models of each structure by reducing noise, smoothing, optimizing, and repairing the model. After applying these tools, relatively smooth and clear feature data were obtained. Using the automatic surface function, the optimized triangular surface model was fitted with a high-precision surface to generate an accurate surface. The model was then converted to CAD objects to generate 3D solid data (**Fig. 2A**), which were exported in STP format for further analysis.

Model Assembly and Construction for Each Varus and Valgus Angle of the Prosthesis

The model of each structural component in STP format was imported into SOLIDWORKS 2017 and assembled according to the coordinates and relative position relationship of each component. Subsequently, a 3D solid model of the knee standard position in UKA was constructed with the relative position of each component, such as bone, cartilage, and prosthesis, fixed.

Using SOLIDWORKS 2017 software, 3D solid models of UKA were constructed based on a standard position model. The position of the tibial lateral prosthesis platform remained unchanged, and the tibial mechanical axis served as the reference point. Subsequently, additional 3 D solid models of UKA were created by introducing femoral prostheses at varus and valgus angles of 2°, 4°, 6°, 8°, 10°, and 12°. These models were then exported in STP format (**Fig. 2B, C**) for further analysis.

Finite Element Modeling and Simulation Analysis

The 3D solid model files in STP format were imported into ANSYS Workbench 2019 software. For finite element modeling, various operations were performed, such as assigning material properties, dividing the mesh, and setting boundary conditions.

The first step was to establish and annotate the material properties corresponding to each structural component of the model, including material name, elastic modulus, Poisson's ratio, and other material parameters[16]. These properties are shown in **Table 1**.

The second step was finite element discretization of the model. The tetrahedral mesh elements were specified for grid division, and the quality of the generated mesh was checked and the convergence was verified. Subsequently, the finite element mesh was subdivided to accurately capture the details of the knee joint model. Finally, boundary conditions were set for the simulation.

Numbers of Structural Nodes and Elements

In this model, there were 298,538 elements and 530,624 nodes in total. The specific elements and nodes of each construction are shown in **Table 2**.

Contact links were created between lateral femur cartilage and lateral meniscus, lateral femur cartilage and lateral tibial plateau cartilage, lateral meniscus and lateral tibial plateau cartilage, femoral prosthesis and a polyethylene gasket, and the polyethylene gasket and tibial plateau prosthesis. The lateral femur and lateral meniscus, as well as the lateral meniscus and lateral tibial plateau cartilage, were defined as binding connections. Frictionless limited sliding surface contact was established between the lateral femoral cartilage and lateral meniscus, as well as between the lateral femoral cartilage and lateral tibial plateau cartilage. Additionally, a frictionless interface was assumed between the femoral prosthesis and the polyethylene gasket.

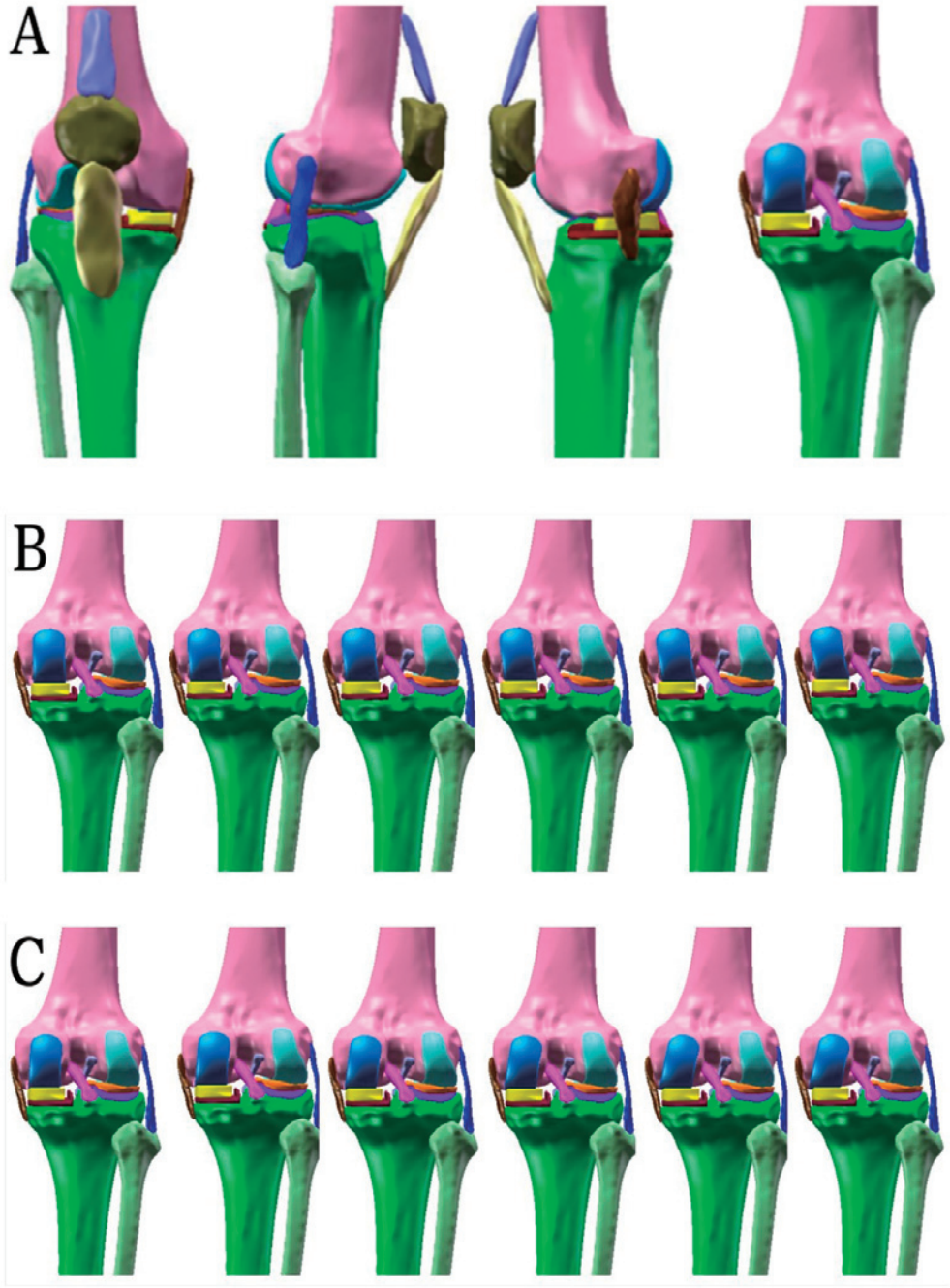

Fig. 2 Finite element models of the femoral prosthesis in standard position and at different varus/valgus angles. **(A)** The standard prosthesis position, namely, varus and valgus angles of 0°. **(B)** From left to right, the position of the femoral prosthesis at varus angles of 2°, 4°, 6°, 8°, 10°, and 12°. **(C)** From left to right, the position of the femoral prosthesis at valgus angles of 2°, 4°, 6°, 8°, 10°, and 12°.

To compare the effect of varus/valgus angles on stress values at the knee joint, the same boundary conditions and loading mode were used for all 13 models, including the standard position (varus/valgus 0°) and models with varus/valgus angles of 2°, 4°, 6°, 8°, 10°, and 12°. To simulate the actual force situation of the UKA model, a fixed restraint was applied at the distal tibial position, and a concentrated force load of 1,000 N was applied at the distal femur along the mechanical axis of the femur toward the distal tibia, as shown in **Figure 3**.

Thirteen types of finite element models were simulated in ANSYS Workbench 2019 software to verify the analytical computational convergence. The results of the stress distribution on the lateral femur cartilage surface, lateral meniscus, and lateral tibial plateau were obtained. The highest stress values were extracted and counted and

Table 1 Material parameters for each tissue structure

Construction	Modulus of elasticity (MPa)	Poisson's ratio
Metal prosthesis	195,000	0.3
Femur	3,884.3	0.3
Tibia	4,184.6	0.3
Fibula	4,164.6	0.3
Polyethylene liner	685	0.4
Meniscus	27.5	0.33
Cartilage	15	0.46
Ligaments	48	0.3

Table 2 Numbers of structural nodes and elements for each structure

Construction	Nodes	Elements
Femoral cartilage	17,001	8,533
Tibial cartilage	11,558	5,816
Femur	161,826	91,746
Tibia	162,651	92,919
Fibula	26,623	15,168
Medial collateral ligament	18,914	10,574
Lateral collateral ligament	13,670	7,552
Cruciate ligament	17,755	9,913
Lateral meniscus	12,662	6,668
Prosthesis	87,964	49,649

Fig. 3 Magnitude and direction of load force.

presented in **Figure 4A～C**.

Accuracy Verification of Finite Element Model of Unicompartmental Knee Arthroplasty

The accuracy of the finite element reference model of the knee joint (femoral prosthesis at varus and varus 0°) was verified by applying a 1,000 N load. The results showed that the highest stress values on the surface of the cartilage of the femoral lateral condyle, the cartilage of the tibial lateral platform, and the lateral meniscus were 4.31 ± 0.06, 2.09 ± 0.06, and 5.58 ± 0.08 Mpa, respectively. These results were similar to those reported in previous studies[17–21], proving that our finite element model was accurate and effective.

Statistical Analysis

All relevant data were collected and used to establish a database. The data were then imported into the SPSS18.0 statistical software system for analysis. The six points with the highest stress were averaged to obtain the highest stress value. The highest stress value was used as the measurement data and showed a normal distribution, expressed as $\bar{x} \pm s$. The t-test was used to compare the highest stress value of each UKA model with that of the standard position model.

Results

This study established finite element models of UKA with the femoral prosthesis at varus/valgus angles of 0°, 2°, 4°, 6°, 8°, 10°, and 12°. The lateral compartment cartilage and lateral meniscus exhibited the highest surface stress values in all models. The values presented in **Table 3** were derived by calculating the mean value from the six stress points with the highest magnitudes. As compared with the femoral prosthesis standard position (varus/valgus angle 0°), the surface stress magnitudes on the lateral femoral condyle cartilage, lateral tibial plateau cartilage, and lateral meniscus were higher when the femoral prosthesis varus/valgus angle was less than 4°($p > 0.05$). In addition, the stress magnitude on the lateral compartment cartilage and lateral meniscus was signifi-

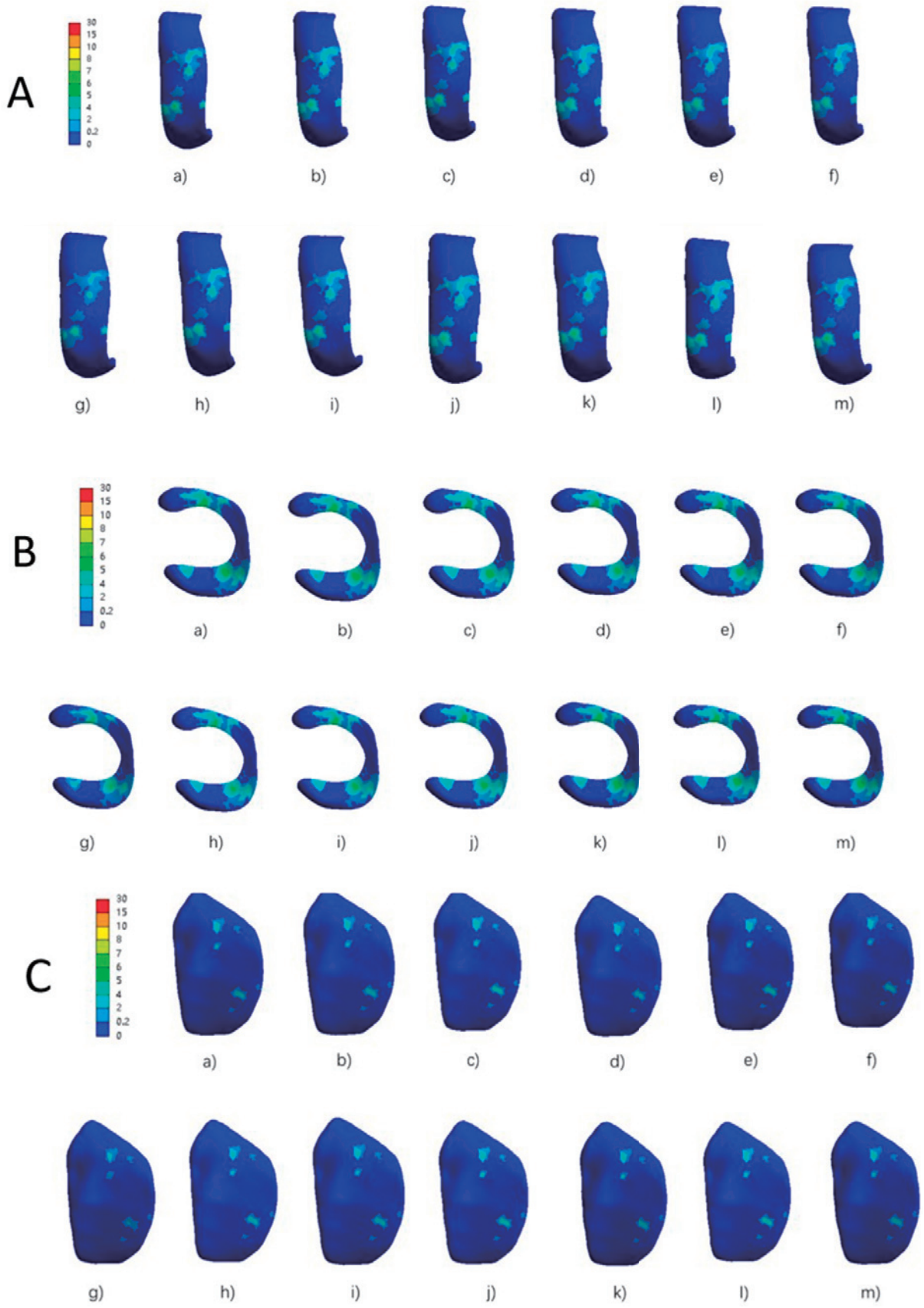

Fig. 4 Stress clouds on the lateral compartment of the knee joint. **(A)** Stress clouds on the cartilage surface of the lateral femoral epicondyle at femoral prosthesis varus/valgus angles of 0°, 2°, 4°, 6°, 8°, 10°, and 12°. **(B)** Stress clouds on the surface of the lateral meniscus at femoral prosthesis varus/valgus angles of 0°, 2°, 4°, 6°, 8°, 10°, and 12°. **(C)** Stress clouds on the surface of the lateral tibial plateau at femoral prosthesis varus/valgus angles of 0°, 2°, 4°, 6°, 8°, 10°, and 12°.

Table 3 Changes in lateral compartment surface stress compared with a varus/valgus angle of 0°

Prosthesis Placement	Maximum Surface Stress (Mpa)					
	Lateral Femoral Condyle Cartilage	*P*-value	Lateral Meniscus	*P*-value	Lateral Tibial Plateau Cartilage	*P*-value
Varus						
12°	5.08±0.08	*P*<0.001	6.57±0.11	*P*<0.001	2.46±0.07	*P*<0.001
10°	4.84±0.07	*P*<0.001	6.45±0.10	*P*<0.001	2.38±0.06	*P*<0.001
8°	4.70±0.11	*P*<0.001	6.32±0.10	*P*<0.001	2.30±0.05	*P*<0.001
6°	4.53±0.07	*P*<0.001	5.99±0.07	*P*<0.001	2.23±0.08	*P*<0.001
4°	4.37±0.07	0.12	5.65±0.08	0.079	2.14±0.06	0.07
2°	4.34±0.09	0.33	5.62±0.09	0.312	2.12±0.07	0.28
Standard Position						
0°	4.31±0.06		5.58±0.08		2.09±0.06	
Valgus						
2°	4.33±0.07	0.30	5.61±0.07	0.447	2.11±0.04	0.45
4°	4.36±0.05	0.20	5.63±0.08	0.207	2.13±0.07	0.14
6°	4.47±0.10	*P*<0.001	5.91±0.07	*P*<0.001	2.21±0.07	*P*<0.001
8°	4.65±0.08	*P*<0.001	6.25±0.10	*P*<0.001	2.29±0.05	*P*<0.001
10°	4.96±0.08	*P*<0.001	6.52±0.08	*P*<0.001	2.40±0.06	*P*<0.001
12°	5.21±0.07	*P*<0.001	6.74±0.09	*P*<0.001	2.52±0.05	*P*<0.001

P<0.05 indicates a significant difference.

Table 4 Changes in medial compartment surface stress compared with a varus/valgus angle of 0°

Prosthesis Placement	Maximum Surface Stress (Mpa)			
	Polyethylene liner	*P*-value	Cancellous bone surface under the tibial prosthesis	*P*-value
Varus				
12°	20.28±1.02	*P*<0.001	3.52±0.10	*P*<0.001
10°	19.15±1.08	*P*<0.001	3.28±0.12	*P*<0.001
8°	18.65±1.03	*P*<0.001	3.22±0.07	*P*<0.001
6°	17.97±1.12	*P*<0.001	3.13±0.08	*P*<0.001
4°	17.45±1.07	0.18	2.97±0.05	0.18
2°	17.14±1.10	0.52	2.95±0.05	0.50
Standard Position				
0°	16.86±1.05		2.93±0.07	
Valgus				
2°	17.21±1.07	0.43	2.96±0.05	0.31
4°	17.58±1.05	0.10	2.98±0.06	0.09
6°	18.17±1.10	*P*<0.001	3.15±0.05	*P*<0.001
8°	18.86±1.09	*P*<0.001	3.23±0.09	*P*<0.001
10°	19.25±1.13	*P*<0.001	3.34±0.07	*P*<0.001
12°	20.47±1.08	*P*<0.001	3.56±0.06	*P*<0.001

P<0.05 indicates a significant difference.

cantly higher at femoral prosthesis varus/valgus angles greater than 4° ($p < 0.001$).

The highest surface stress values on the polyethylene liner and cancellous bone surface under the tibial prosthesis were recorded in detail for all models, as shown in **Table 4**. As compared with the femoral prosthesis standard position (varus/valgus angle 0°), the surface stress magnitudes on the polyethylene liner and cancellous bone surface under the tibial prosthesis were significantly higher at femoral prosthesis varus/valgus angles greater than 4° ($p < 0.001$).

Changes in Stress on the Cartilage Surface of the Lateral Compartmental in Different UKA Models

As shown in **Figure 5A**, at femoral prosthesis varus/

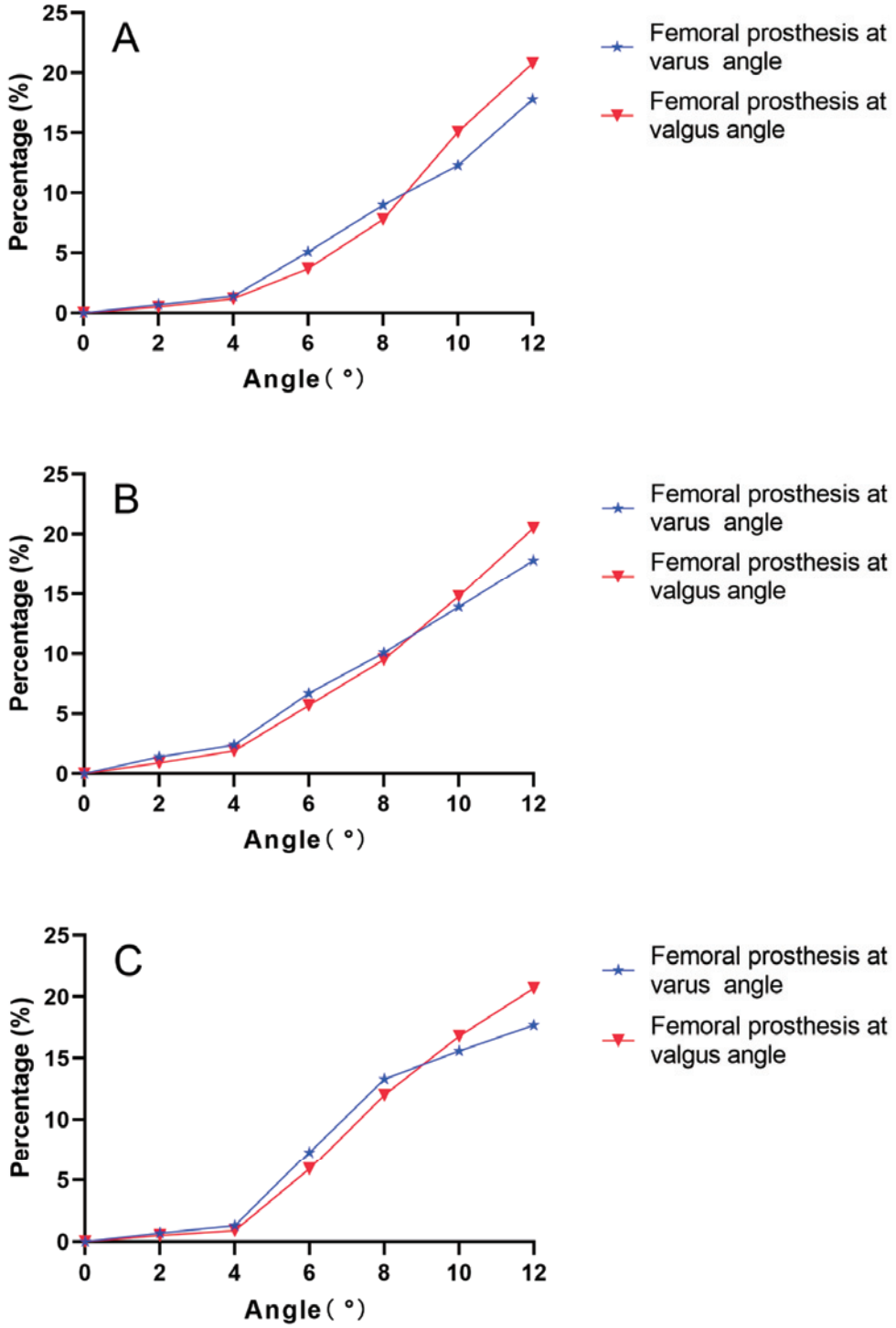

Fig. 5 Percentage change in surface stress values on the lateral compartment cartilage and meniscus at different femoral prosthesis varus/valgus angles. **(A)** Percentage change in surface stress on the lateral femoral condyle cartilage. **(B)** Percentage change in surface stress on the lateral tibial plateau cartilage. **(C)** Percentage change in surface stress on the lateral meniscus.

valgus angles of 0°, 2°, 4°, 6°, 8°, 10°, and 12°, the surface stress magnitudes on the lateral femoral condyle cartilage were 0.7%/0.5%, 1.4%/1.2%, 5.1%/3.7%, 9.0%/7.8%, 12.3%/15.1%, and 17.8%/20.8% higher, respectively, than those of the standard position. Moreover, at these angles, the surface stress magnitudes of the lateral tibial plateau cartilage were 1.4%/0.9%, 2.4%/1.9%, 6.7%/5.7%, 10.1%/9.5%, 13.9%/14.8%, and 17.8%/20.5% higher, respectively, than those of the standard position, as shown in **Figure 5 B**. The stress magnitude on the lateral compartment carti-

lage was significantly higher at varus/valgus angles greater than 4° ($p < 0.001$).

As shown in **Figure 5C**, at femoral prosthesis varus/valgus angles of 2°, 4°, 6°, 8°, 10°, and 12°, the surface stress magnitudes on the lateral meniscus were 0.7%/0.5%, 1.3%/0.9%, 7.3%/5.9%, 13.3%/12.0%, 15.6%/16.8%, and 17.7%/20.7% higher, respectively, than those of the standard position. The stress magnitude on the lateral meniscus was significantly higher at a varus/valgus angle greater than 4° ($p < 0.001$).

Discussion

Studies have demonstrated that FEA is a highly accurate and repeatable method for simulating the kinematics of the knee joint and for accurately reflecting the magnitude and distribution of stress within the joint[22–24]. However, the potential clinical utility of this approach has been compromised by the improper selection of research subjects in previous studies. For example, Kwon et al.[25] and Park et al.[26] selected a healthy mature male and a healthy mature male athlete with no prior history of knee injury as research subjects for FEA. However, since the goal is to analyze changes in knee joint biomechanics, the results obtained from FEA of healthy knee joints may not accurately reflect the knee biomechanics of people with knee osteoarthritis. Therefore, these experimental results lack reliability. Thus, it is necessary to adopt a more accurate FEA modeling method to study changes in knee biomechanics after a surgical procedure. The primary objective of FEA is to investigate the biomechanical alterations occurring in knee joints after UKA. Hence, it is more consistent with the goals of FEA to choose patients who have undergone UKA as research subjects, rather than selecting healthy individuals. Previous studies have demonstrated the reliability of selecting post-UKA patients as subjects for FEA investigations. Sasatani et al.[27] selected a medial osteoarthritic knee for FEA. Srinivas et al.[28] used FEA to investigate five patients who underwent TKA. Therefore, we selected one post-UKA patient for FEA, to study the effects of a femoral prosthesis placed at different varus/valgus angles on changes in knee biomechanics, which provided more reliable and accurate results.

Recently, several studies of healthy adult volunteers analyzed the placement position of the tibial prosthesis in mobile-bearing UKA. Ma et al.[29] established the normal knee joint and fixed-bearing UKA models with different femoral prosthesis varus and valgus angles. They found that the high-stress magnitude on the lateral compartment cartilage surface increased at varus positions but decreased at valgus positions. Innocenti et al.[30] pointed out that the tibial prosthesis of the fixed platform should have either no varus and valgus angle or have a varus and valgus angle greater than 3°. Kang et al.[31] found that 5-7° is the optimal range of the caster angle for fixed platform tibial prosthesis; higher and lower values accelerated the wear of cartilage and polyethylene. Gaudiani et al.[32] found that, in the placement of the UKA prosthesis, a varus and valgus angle of 1-4° achieved good clinical results, whereas a varus and valgus angle greater than 5° aggravated degeneration of the contralateral compartment and caused early loosening of the prosthesis. Kim et al.[33] postulated that overcorrection of the lower limb force line during UKA (valgus force line exceeding 180°) may lead to progression of contralateral intercompartment osteoarthritis of the knee.

In our study, we found that the stress values on the articular cartilage surface of the femoral lateral condyle, tibial lateral platform, and lateral meniscus surface gradually increased as the femoral prosthesis varus/valgus angle increased. As compared with the femoral prosthesis standard position (varus/valgus angle 0°), surface stress values on the lateral femoral condyle cartilage, lateral tibial plateau cartilage, and lateral meniscus were higher when the femoral prosthesis varus/valgus angle was less than 4° ($p > 0.05$). In addition, the stress magnitude on the lateral compartment cartilage and lateral meniscus significantly increased when the femoral prosthesis varus/valgus angle was greater than 4° ($p < 0.001$). These results were consistent with the conclusions drawn by Gaudiani et al.[32] and Kang et al.[34] We speculate that this phenomenon may be caused by the improper placement angle of the femoral prosthesis. Specifically, a femoral prosthesis varus/valgus angle exceeding 6° may have increased the risk of adverse biomechanical changes in the lateral compartment cartilage and meniscus, thereby worsening the overall clinical outcomes of patients. However, our findings are inconsistent with results reported by Ma et al.[29], perhaps because of differences in the patients analyzed by FEA. Because Ma et al. chose healthy adult volunteers for FEA, their results lack reliability.

Our study revealed that the surface stress values on both the polyethylene liner and cancellous bone beneath the tibial prosthesis increased with an increasing femoral prosthesis varus/valgus angle. Specifically, as compared with the standard position of the femoral prosthesis (varus/valgus angle 0°), the surface stress values on the polyethylene liner and cancellous bone were higher when the femoral prosthesis varus/valgus angle was less

than 4°, although statistical significance was not reached ($p > 0.05$). However, stress magnitudes on the polyethylene liner and cancellous bone beneath the tibial prosthesis were significantly higher when the femoral prosthesis varus/valgus angle exceeded 4° ($p < 0.001$). This notable increase in stress could potentially accelerate polyethylene liner wear and contribute to tibial prosthesis loosening. Furthermore, we observed that when the femoral prosthesis was placed in a valgus position rather than a varus position the surface stress values on the polyethylene liner and cancellous bone beneath the tibial prosthesis were higher. This observation is likely attributable to a combination of factors, including reduced stress sharing by the medial cortical bone in the valgus position of the femoral prosthesis, external displacement of the tibial prosthesis force point, and an increased load on the medial compartment.

This study has some limitations. First, although the finite element model of the present post-UKA patient ensured comparability with other models, the results lacked group representation. A more complete finite element model should be established in future research. In addition, this study was subject to the constraint of utilizing a single finite element model. To achieve a more comprehensive understanding of the biomechanical alterations of the femoral prosthesis at various varus/valgus angles, it would be beneficial to use multiple finite element models, considering different varus/valgus angles and caster angles of the tibial prosthesis. Such an approach would facilitate a deeper investigation of the biomechanical changes and their implications.

Conclusions

The FEA model was used to analyze surface stress magnitudes on the lateral femoral condyle cartilage, lateral tibial plateau cartilage, and lateral meniscus after UKA. The results indicated that the optimal position of the femoral prosthesis varus/valgus angle in UKA was less than 4°.

Acknowledgements: Thanks to all the contributors and participants. The authors would like to thank all the reviewers who participated in the review, as well as MJEditor (www.mjeditor.com) for providing English editing services during the preparation of this manuscript.

Funding: This study was supported by the Science and Technology Projects in the Field of Health, Xiangyang City (2022 YL33A).

Conflict of Interest: The authors declare no conflict of interest.

References

1. Smith WB 2nd, Steinberg J, Scholtes S, Mcnamara IR. Medial compartment knee osteoarthritis: age-stratified cost-effectiveness of total knee arthroplasty, unicompartmental knee arthroplasty, and high tibial osteotomy. Knee Surg Sports Traumatol Arthrosc. 2017;25(3):924–33.
2. Santoso MB, Wu L. Unicompartmental knee arthroplasty, was it superior to high tibial osteotomy in treating unicompartmental osteoarthritis? A meta-analysis and systemic review. J Orthop Surg Res. 2017;12(1):50.
3. Siman H, Kamath AF, Carrillo N, Harmsen WS, Pagnano MW, Sierra RJ. Unicompartmental knee arthroplasty vs total knee arthroplasty for medial compartment arthritis in patients older than 75 years: Comparable reoperation, revision, and complication rates. J Arthroplasty. 2017;32 (6):1792–7.
4. Weber P, Schroder C, Schmidutz F, et al. Increase of tibial slope reduces backside wear in medial mobile bearing unicompartmental knee arthroplasty. Clin Biomech (Bristol, Avon). 2013;28(8):904–9.
5. Quilez MP, Seral B, Perez MA. Biomechanical evaluation of tibial bone adaptation after revision total knee arthoplasty: A comparison of different implant systems. PLoS One. 2017;12(9):e0184361.
6. Winnock de Grave P, Barbier J, Luyckx T, Ryckaert A, Gunst P, Van den Daelen L. Outcomes of a fixed-bearing, medial, cemented unicondylar knee arthroplasty design: Survival analysis and functional score of 460 cases. J Arthroplasty. 2018;33:2792–9.
7. Hansen EN, Ong KL, Lau E, Kurtz SM, Lonner JH. Unicondylar knee arthroplasty has fewer complications but higher revision rates than total knee arthroplasty in a study of large United States databases. J Arthroplasty. 2019;34(8):1617–25.
8. Pandit H, Jenkins C, Gill HS, Barker K, Dodd CA, Murray DW. Minimally invasive Oxford phase 3 unicompartmental knee replacement: results of 1000 cases. J Bone Joint Surg Br. 2011;93(2):198–204.
9. Koshino T, Sato K, Umemoto Y, Akamatsu Y, Kumagai K, Saito T. Clinical results of unicompartmental arthroplasty for knee osteoarthritis using a tibial component with screw fixation. Int Orthop. 2015;39(6):1085–91.
10. Tan MWP, Ng SWL, Chen JY, Liow MHL, Lo NN, Yeo SJ. Long-term functional outcomes and quality of life at minimum 10-year follow-up after fixed-bearing unicompartmental knee arthroplasty and total knee arthroplasty for isolated medial compartment osteoarthritis. J Arthroplasty. 2021;36(4):1269–76.
11. Kwon OR, Kang KT, Son J, Suh DS, Baek C, Koh YG. Importance of joint line preservation in unicompartmental knee arthroplasty: Finite element analysis. J Orthop Res. 2017;35(2):347–52.
12. Sawatari T, Tsumura H, Iesaka K, Furushiro Y, Torisu T. Three-dimensional finite element analysis of unicompartmental knee arthroplasty--the influence of tibial component inclination. J Orthop Res. 2005;23(3):549–54.
13. Koh YG, Park KM, Kang KT. Finite element study on the preservation of normal knee kinematics with respect to the prosthetic design in patient-specific medial unicompartmental knee arthroplasty. Biomed Res Int. 2020;2020: 1829385.
14. Inoue S, Akagi M, Asada S, Mori S, Zaima H, Hashida M.

The valgus inclination of the tibial component increases the risk of medial tibial condylar fractures in unicompartmental knee arthroplasty. J Arthroplasty. 2016;31(9):2025–30.
15. Zhu GD, Guo WS, Zhang QD, Liu ZH, Cheng LM. Finite element analysis of mobile-bearing unicompartmental knee arthroplasty: The influence of tibial component coronal alignment. Chin Med J (Engl). 2015;128(21):2873–8.
16. Giffin JR, Vogrin TM, Zantop T, Woo SL, Harner CD. Effects of increasing tibial slope on the biomechanics of the knee. Am J Sports Med. 2004;32(2):376–82.
17. Iesaka K, Tsumura H, Sonoda H, Sawatari T, Takasita M, Torisu T. The effects of tibial component inclination on bone stress after unicompartmental knee arthroplasty. J Biomech. 2002;35(7):969–74.
18. Song Y, Debski RE, Musahl V, Thomas M, Woo SL. A three-dimensional finite element model of the human anterior cruciate ligament: A computational analysis with experimental validation. J Biomech. 2004;37(3):383–90.
19. Kim KT, Lee S, Lee JI, Kim JW. Analysis and treatment of complications after unicompartmental knee arthroplasty. Knee Surg Relat Res. 2016;28(1):46–54.
20. Li G, Meng H, Liu J, Zou D, Li K. A novel modeling approach for finite element human body models with high computational efficiency and stability: Application in pedestrian safety analysis. Acta Bioeng Biomech. 2021;23(2):33–40.
21. Vandana KL, Deepti M, Shaimaa M, Naveen K, Rajendra D. A finite element study to determine the occurrence of abfraction and displacement due to various occlusal forces and with different alveolar bone height. J Indian Soc Periodontol. 2016;20(1):12–6.
22. Castiello E, Affatato S. Progression of osteoarthritis and reoperation in unicompartmental knee arthroplasty: A comparison of national joint registries. Int J Artif Organs. 2020;43(3):203–7.
23. Chun YM, Kim SJ, Kim HS. Evaluation of the mechanical properties of posterolateral structures and supporting posterolateral instability of the knee. J Orthop Res. 2008;26(10):1371–6.
24. Scott CE, Eaton MJ, Nutton RW, Wade FA, Evans SL, Pankaj P. Metal-backed versus all-polyethylene unicompartmental knee arthroplasty: Proximal tibial strain in an experimentally validated finite element model. Bone Joint Res. 2017;6(1):22–30.
25. Kwon HM, Lee JA, Koh YG, Park KK, Kang KT. Effects of contact stress on patellarfemoral joint and quadriceps force in fixed and mobile-bearing medial unicompartmental knee arthroplasty. J Orthop Surg Res. 2020;15(1):517.
26. Park KK, Koh YG, Park KM, Park JH, Kang KT. Biomechanical effect with respect to the sagittal positioning of the femoral component in unicompartmental knee arthroplasty. Biomed mater Eng. 2019;30(2):171–82.
27. Sasatani K, Majima T, Murase K, et al. Three-Dimensional Finite analysis of the optimal alignment of the tibial implant in unicompartmental knee arthroplasty. J Nippon Med Sch. 2019;87(2):60–5.
28. Srinivas G R, Deb A, Kumar M N. A study on polyethylene stresses in mobile-bearing and fixed-bearing total knee arthroplasty (TKA) using explicit finite element analysis. J Long Term Eff Med Implants. 2013;23(4):275–83.
29. Ma PC, Zhang SP, Sun RX, Chai H, Jiang K. Biomechanical effects of different placement of femoral prosthesis in unicompartmental knee arthroplasty. Chinese Journal of Tissue Engineering Research. 2022;12(26):1843–8.
30. Innocenti B, Pianigiani S, Ramundo G, Thienpont E. Biomechanical effects of different varus and valgus alignments in medial unicompartmental knee arthroplasty. J Arthroplasty. 2016;31(12):2685–91.
31. Kang KT, Park JH, Koh YG, Shin J, Park KK. Biomechanical effects of posterior tibial slope on unicompartmental knee arthroplasty using finite element analysis. Biomed Mater Eng. 2019;30(2):133–44.
32. Gaudiani MA, Nwachukwu BU, Baviskar JV, Sharma M, Ranawat AS. Optimization of sagittal and coronal planes with robotic-assisted unicompartmental knee arthroplasty. Knee. 2017;24(4):837–43.
33. Kim KT, Lee S, Kim TW, Lee JS, Boo KH. The influence of postoperative tibiofemoral alignment on the clinical results of unicompartmental knee arthroplasty. Knee Surg Relat Res. 2012;24(2):85–90.
34. Kang KT, Son J, Baek C, Kwon OR, Koh YG. Femoral component alignment in unicompartmental knee arthroplasty leads to biomechanical change in contact stress and collateral ligament force in knee joint. Arch Orthop Trauma Surg. 2018;138(4):563–72.

(Received, March 22, 2023)
(Accepted, August 9, 2023)